

Numerical modeling and design optimization of a concentrated solar thermal collector for dry methane reforming

Shomik Verma, Nico Hotz

Thermodynamics and Sustainable Energy Laboratory, Pratt School of Engineering,
Duke University, Durham, NC, USA

Abstract

This study details the modeling of a solar thermal collector designed to maximize absorption of solar heat. The heat is used to drive a dry methane reforming reaction to produce H_2 and CO from CH_4 and CO_2 . The finite element method based numerical model takes into account all modes of heat transfer, fluid flow, and chemical reaction. The goal of this study was to improve a previously designed collector to optimize absorber temperature. Various operational parameters were varied to obtain the final simulated results of optimized collector design. Different tube materials were considered to improve insulation given the high temperatures of the collector. Catalyst characteristics were tuned to accurately match experimental data. Absorption coating optical properties were optimized to maximize temperature. The results show a vacuum-insulated, high-temperature solar thermal collector for dry methane reforming can be manufactured, and is capable of achieving high temperatures even with low concentration ratios.

Introduction

There have been tremendous efforts in recent years to develop solar technologies to absorb energy from the sun more effectively [1]. One method is solar photovoltaics, which converts sunlight directly to electricity [1]. However, this methodology is associated with several difficulties. First, typical commercial photovoltaics can only absorb a fraction of incident sunlight, limiting their efficiency to ~20% [2]. Additionally, storing electricity is problematic, as batteries are net negative (the amount of energy inputted is greater than the amount that can be drawn) and have low energy density [3].

Therefore, this study aims to develop a solar thermal collector that absorbs solar heat rather than sunlight. We are thus able to absorb a wider range of the solar spectrum, increasing the overall efficiency of the system [4]. The key to harnessing solar heat is selective absorption: high absorptivity in the ultraviolet (UV) and visible regions and low emissivity in the infrared (IR) region. This allows both absorption and retention of heat, allowing the collector to achieve high temperatures. An ideal collector would have 100% visible absorption and 0% IR emission, shown in Figure 1 below [5].

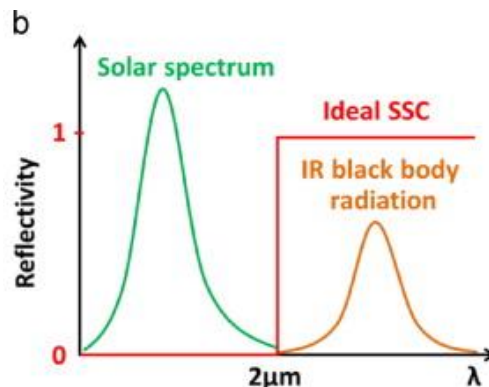


Figure 1: Example of the ideal solar selective coating with 0 UV/visible reflectivity (100% absorption) and 1 IR reflectivity (0% emission).

However, even the best solar selective absorbers are unable to achieve high temperatures (>1000 K) [6]. To attain these temperatures, concentrated solar power (CSP) is required. By installing an array of mirrors or a lens, we are able to concentrate sunlight to achieve much higher than the 1000 W/m^2 normal incident power density [4]. This allows our collector to reach higher temperatures through higher heat flux.

There are various ways to store this heat. Some common systems use molten salt for thermal energy storage [7]. However, these methodologies require heavily insulation to prevent heat loss. Our methodology of storage is through chemical reaction. Many reactions use heat to convert products to reactants, serving as a storage mechanism for this heat. In choosing the chemical reaction best suited for solar input, we turn to another common problem: hydrogen generation. Currently, the majority of hydrogen is produced through steam reforming [8], which reacts natural gas (primarily methane) with steam in industrial furnaces to produce H_2 and CO , known as syngas. Additional H_2 can be produced through the water-gas shift reaction [8]. These 2 reactions are described below.



Reaction set 1: Steam methane reforming (SMR) and water-gas shift (WGS) reactions. SMR is highly endothermic while WGS is mildly exothermic.

However, this process wastes methane, as the industrial furnaces usually burn about 50% of the natural gas to provide the heat of reaction [8]. Instead, we propose to use solar energy as the heat input, making the process more sustainable. We also use biofuel-based methane as the chemical input instead of natural gas, making the process carbon neutral as it only emits the CO₂ consumed when the plants were growing. Additionally, instead of using steam reforming, we propose the dry reforming reaction, which uses CO₂ instead of steam to help form syngas [9].



Reaction set 2: Dry methane reforming (DMR) and reverse water-gas shift (RWGS) reactions. RWGS may have a lower activation energy than DMR.

Thus, 2 potent greenhouse gases, methane and CO₂, are combined to form an immensely useful gas: hydrogen. The biggest problem with this method is that hydrogen production may be limited by a different reaction, the reverse water-gas shift reaction, which reacts the produced H₂ with existing CO₂ to form additional CO [10]. Typically, the activation energy for RWGS is lower than DMR. However, at higher temperatures, the activation energy for RWGS increases, while the activation energy for DMR decreases [11]. Additionally, catalysts can be created to selectively react methane without activating the RWGS reaction [12]. Therefore, DMR is an attractive reaction for chemical storage of heat in a high-temperature concentrated solar collector.

Our numerical simulation therefore models the operation of a concentrated solar collector for dry methane reforming. The geometry of the model is shown below.

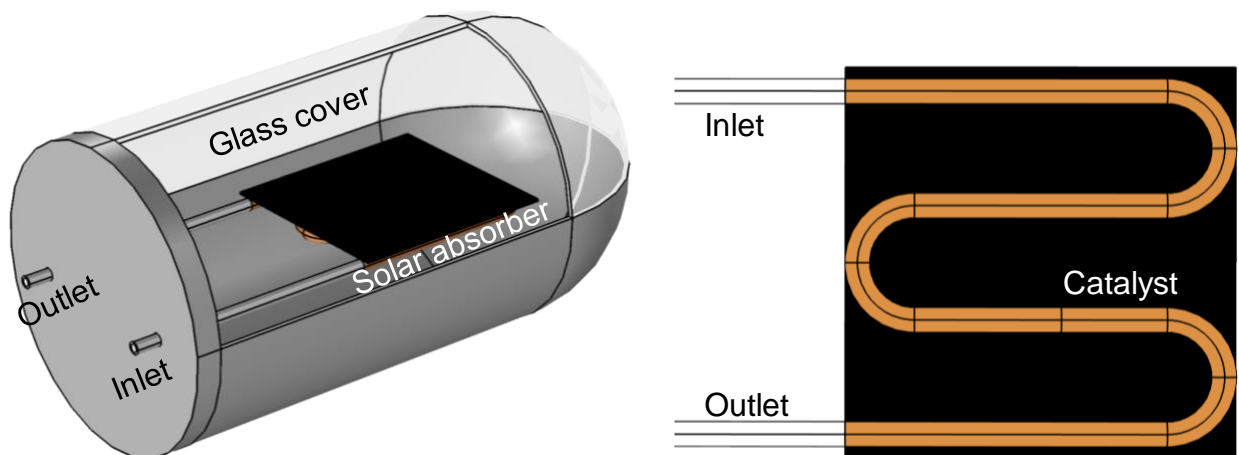


Figure 2: (left) Complete model of vacuum-insulated collector with glass cover and steel bulkhead. (right) Tube layout below copper collector coated with selective absorber.

The collector consists of one inlet and one outlet tube, both connected to the bulkhead on the side of the collector to prevent issues with thermal expansion. The tubes wind around the copper collector, which is coated with a selective absorber on both sides. The fluid flow through the tubes is heated through contact with this solar absorber. Flow is then reacted by passing through a packed bed reactor with catalyst that is located after the 2nd bend of the tube. The products then flow to the outlet. This system is enclosed in a glass cover which is pumped down to a vacuum. For the purposes of the simulation, a perfect vacuum is assumed - in reality the pressure is reduced to ~2 mTorr.

The original collector design was proposed by Real et al. [13]. However, this collector was designed for methanol reforming, which occurs at much lower temperatures (~500 K). The design must be updated for the high temperatures (~1000K) of dry methane reforming. Specifically, the tube materials used must be changed to improve the insulation and reduce heat losses. Additionally, the optical properties of the selective absorber must be optimized again. This includes adjusting the cutoff wavelength for high absorptivity/low emissivity, and determining the selectivity required.

This study aims to model and optimize this new concentrated solar thermal collector. Starting from the original design, various parameters were updated to maximize the coating temperature and conversion of CH₄ to H₂. The following sections detail the computational methods used to model the collector, and the results obtained from these methods. The conclusions from this simulation will be used to manufacture a new solar collector that is better suited for high-temperature operation. Manufacturing of a physical prototype will also allow experimental verification of the simulated results presented here.

Computational Methods

To accurately model the collector, multiple physics interfaces must be considered, including heat transfer, fluid flow, and chemical reaction. The heat transfer interface must include surface-to-surface radiation to account for the heat absorption and emission of the selective coating. The fluid flow is considered laminar, and set to 10 SCCM for the optimization. Heat transfer and fluid flow are coupled through isothermal flow.

The chemical reaction impacts both fluid flow and heat transfer. The inlet condition is 50% mole fraction each for CH₄ and CO₂. The reaction creates products with lower density than the reactants, influencing the laminar flow velocity and pressure. The laminar flow velocity also determines residence time of the reactants and hence conversion, further coupling laminar flow and reaction. The reaction is also endothermic and requires continuous heat input, thus coupling heat transfer and chemical reaction.

Therefore, the COMSOL Physics interfaces used were Heat Transfer, Fluid Flow, Transport of Concentrated Species, and Chemistry. Non-isothermal Flow and Reacting Flow Multiphysics were used to properly couple the various physics.

The heat transfer equations used are described below.

$$\mathbf{q} = -k\nabla T \quad (1)$$

$$\rho c_p \mathbf{u} \cdot \nabla T + \nabla \cdot \mathbf{q} = Q \quad (2)$$

$$q = \int_0^\infty \epsilon(\lambda) \sigma (T_1^4 - T_2^4) d\lambda \quad (3)$$

Where q is the heat flux, k is the thermal conductivity (W/m²K), T is the temperature (K), ρ is the density (kg/m³), c_p is the specific heat (J/K), u is the velocity field (m/s), Q is the heat source (W/m³), ϵ is the emissivity, λ is wavelength (nm), σ is the Stefan-Boltzmann constant (W/m²K⁴). Equation 1 describes heat transfer in a solid, due solely to conduction. Equation 2 describes heat transfer in fluids, due to both conduction and convection. It is already evident that multiple physics are coupled – there is a term for velocity field in the heat transfer equation. Radiative heat transfer is also considered, as shown in Equation 3.

Radiation is most important when modeling the selective absorption coating, which has different emissivities as a function of wavelength. As shown in Figure 1, there are two separate emissivities – solar spectrum (UV/visible) and ambient spectrum (IR). Therefore, the solar/ambient emission option was chosen for surface-to-surface radiation to accurately model the coating. The cutoff wavelength (shown in Figure 1 as 2 μm) was varied to find the optimum. Additionally, the selectivity (defined as solar absorptivity over ambient emissivity) was varied to determine how effective the coating must be.

Radiation could also be important if the fluid flow was participating – however, this is difficult to model as: (1) the media is changing due to reaction, and (2) the absorption coefficient of different species varies across several orders of magnitude as a function of wavelength. Therefore, the media was assumed to be non-participating.

The laminar flow equations used are described below:

$$\rho(\mathbf{u} \cdot \nabla)\mathbf{u} = \nabla \cdot [-p\mathbf{I} + \mu(\nabla\mathbf{u} + (\nabla\mathbf{u})^T) - \frac{2}{3}\mu(\nabla \cdot \mathbf{u})\mathbf{I}] + \mathbf{F} \quad (4)$$

$$\nabla \cdot (\rho\mathbf{u}) = 0 \quad (5)$$

Where \mathbf{I} is the identity tensor, μ is the dynamic viscosity (Pa s), p is the pressure (Pa), and \mathbf{F} is any external forces (N). Equation 4 is the steady-state Navier-Stokes equation for compressible Newtonian fluids with terms corresponding to the inertial forces, pressure forces, viscous forces, and external forces. This equation represents the conservation of momentum. Equation 5 is the steady-state continuity equation representing conservation of mass.

Weakly compressible flow was chosen as the velocities considered were low. The density changed with flow length due to temperature gradient in the tubes, as well as reaction producing species with lower density. Thus, the laminar flow is clearly coupled with both heat transfer and chemical reaction.

The chemical reaction equations used are described below:

$$\mathbf{N}_i = \mathbf{j}_i + \rho\mathbf{u}\omega_i \quad (6)$$

$$\nabla \cdot \mathbf{j}_i + \rho(\mathbf{u} \cdot \nabla)\omega_i = R_i \quad (7)$$

$$R_i = \nu_i \left[A^f \exp\left(\frac{-E^f}{RT}\right) \right] \prod_{i=1}^{Q_r} c_i^{\nu_i} \quad (8)$$

Where \mathbf{N}_i is the total flux, \mathbf{j}_i is the diffusive flux, ω_i is the local mass fraction, R_i is the net volumetric source, ν_i is the stoichiometric coefficient/reaction order, A^f is the forward reaction Arrhenius pre-exponential constant, E^f is the forward reaction activation energy, R is the ideal gas constant, and Q_r is the number of reactants. The subscript i signifies different equation for each species.

Equation 6 details both sources of mass transport, diffusion and convection. Equation 7 is the steady-state convection-diffusion equation. Equation 8 calculates the volumetric source or sink due to reaction, based on the rate constant calculated from the Arrhenius equation, reactant concentration, and reaction order. These equations are coupled to heat transfer directly from the temperature term in Equation 8 and also through density, and coupled to laminar flow due to the velocity field term.

A_f and E_f had to be tuned to our specific catalyst, so experimental data was used to determine these values. The dry methane reforming reaction is known to be first order [14], so the stoichiometric coefficients were the same as the reaction order.

These 3 sets of equations were defined in COMSOL by using the following 4 physics interfaces: Heat Transfer, Laminar Flow, Transport of Concentrated Species, and Chemistry. The 4 physics interfaces were coupled with the Non-isothermal Flow and Reacting Flow multiphysics interfaces, which coupled velocity, density, and temperature across the physics interfaces.

Results

Materials Analysis

As discussed previously, the original collector design used copper tubes to connect the absorber with the steel bulkhead [13]. However, this becomes problematic with the higher temperatures characteristic of a concentrated solar collector – more of the heat can escape from the absorber region to the bulkhead. This problem is compounded with the thermal short circuit created by the looped entry-exit designed to prevent problems due to thermal expansion. Therefore, better insulating materials were considered for the tube material connecting the absorber with the bulkhead. The numerical model was run with a concentration ratio (CR) of 20, creating temperatures of the absorber coating of around 1000K. Materials of various thermal conductivities were considered, ranging from 400 to 1.4 W/mK. The results of this analysis are shown below.

Table 1: Results of material selection for tube connecting absorber with steel bulkhead. Materials with various thermal conductivities are considered.

Material	Thermal Cond (W/mK)	Coating Temp (K)
Copper	400	971.9
Aluminum	238	988.9
Steel	44.5	1011.2
Alumina	27.0	1013.4
Silica Glass	1.38	1017.1

As is expected, materials with a lower thermal conductivity are better insulators and allow more of the heat to remain in the absorber section. However, it is difficult for these insulators to be securely connected to the bulkhead due to their brittleness. Because the collector is vacuum sealed, specialty connectors must be used to prevent leakage. Alumina tubes were chosen due to their ability to be connected with relative ease. Additional reductions in thermal conductivity only marginally improve performance. Figure 3 below shows the temperature distribution when using alumina tubes.

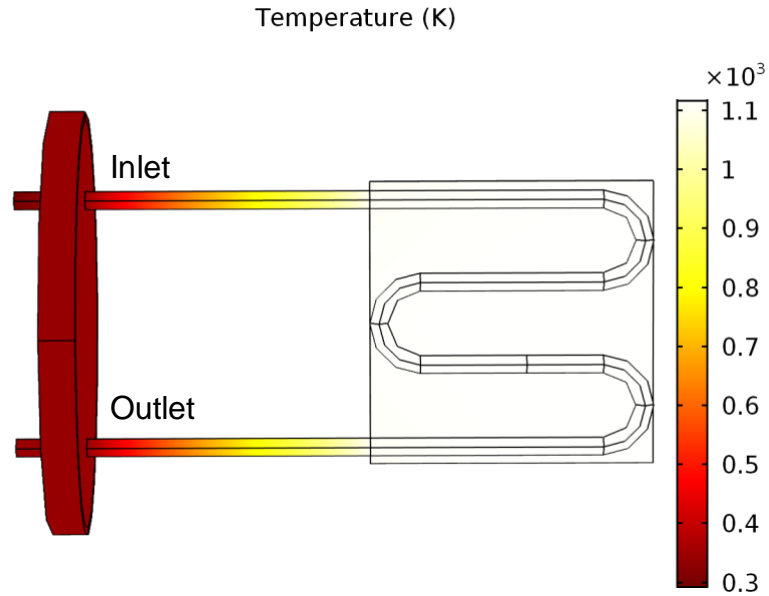


Figure 3: Temperature (K) profile of absorber and bulkhead when using alumina tubes. As is evident, the material prevents heat from escaping to the bulkhead.

It is evident that the alumina tubes help the heat remain in the absorber section of the collector. Now that the insulation material is optimized, it is possible to conduct more rigorous catalyst characterization.

Catalytic Reaction Tuning

Instead of modeling the packed bed reactor as a porous media with heterogeneous reactions, the reactor was modeled as a simple control volume with homogeneous chemical reaction. This helped improve computation time, but required tuning of the catalyst variables to match experimental data [14]. Experimental data was provided matching wall temperature with percent conversion of the two reactants. A separate model was created to expedite the tuning process. The pre-exponential constant A_f and the activation energy E_f were varied across several values until the CH_4 and CO_2 conversions matched data. The final values were:

$$E_f = 90 \frac{\text{kJ}}{\text{mol}}, \quad A_f = 5e5 \frac{\text{m}^3}{\text{mol s}}$$

The following figure shows the mass fraction profile of CH_4 . At the inlet, the mass fraction is 0.26, corresponding to a 50% mole fraction of CH_4 . The CH_4 quickly reacts within the packed catalyst bed, with a mass fraction of less than 0.08 at the outlet.

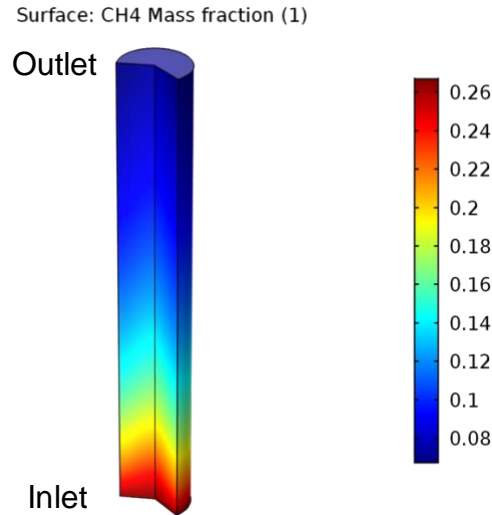


Figure 4: Separate control volume homogeneous reactor model to tune pre-exponential constant and activation energy in full collector model. Shows reduction of CH₄ mass fraction as it reacts with CO₂ to form H₂ and CO.

After tuning the catalyst, the catalyst properties were inputted to the actual model to determine how the collector would function with the given catalyst properties. The following figure shows the mass fraction profile of CH₄ for the modeled collector with CR of 20, creating coating temperature around 1000K.

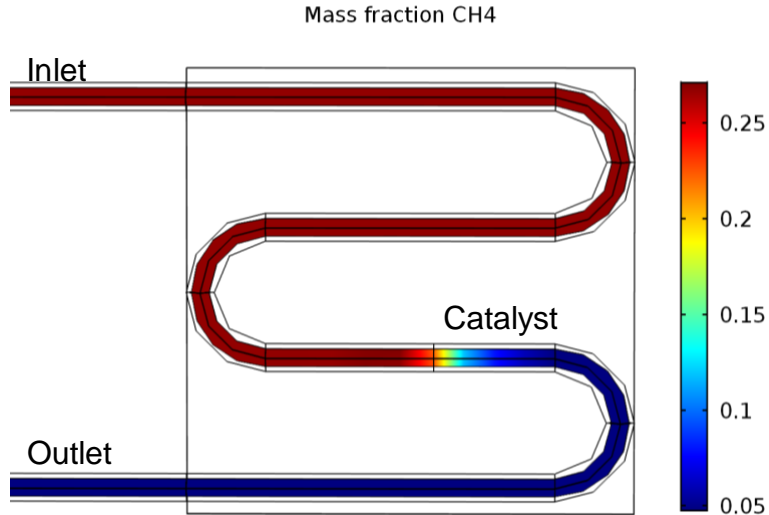


Figure 5: CH₄ mass fraction profile with tuned catalyst properties, showing conversion of CH₄ to products of the reaction.

As is evident, the collector functions effectively with high percent conversion of CH₄. To optimize the collector further, we recall that the heat absorption is contingent upon the optical properties of the absorption coating. Therefore, absorption coating optimization is critical to collector performance.

Absorption Coating Properties

High-temperature solar selective absorption coatings are difficult to fabricate, so their properties should be determined before fabrication. Our application of dry methane reforming occurs best at temperatures around 1000K. To achieve this temperature, a CR of 20 is required. However, lower concentrations could be possible if the optical properties of the absorption coating are optimized. First, the cutoff frequency between high solar absorption and low ambient emissivity was varied.

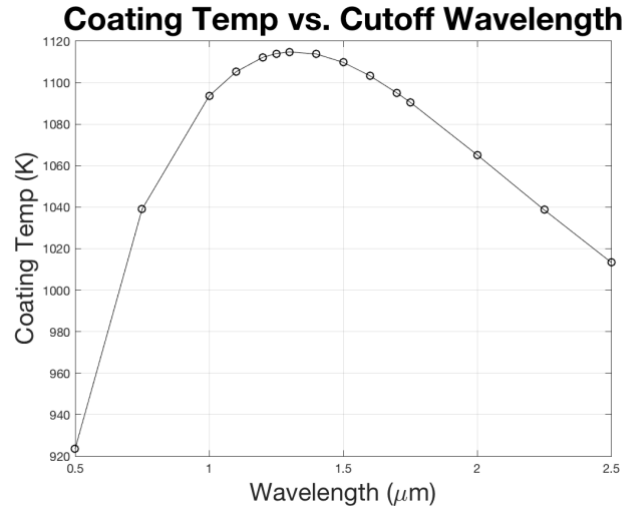


Figure 6: Coating temperature variation as a function of cutoff wavelength, showing a peak at 1.3 μm .

Although using the default 2.5 μm results in a coating temperature of 1018 K, optimizing this value to 1.3 μm increases the temperature by 100 K. This ~10% improvement shows the significance of properly designed absorption coatings.

The second important property of solar selective absorption coatings is the selectivity of the coating. For all of the previous analysis, a solar absorptivity of 0.95 and ambient emissivity of 0.05 was chosen, giving a selectivity of $\frac{0.95}{0.05} = 19$. Typical selective coatings have selectivities in this range. However, improving the selectivity can improve the performance of the collector, as shown in the figure below.

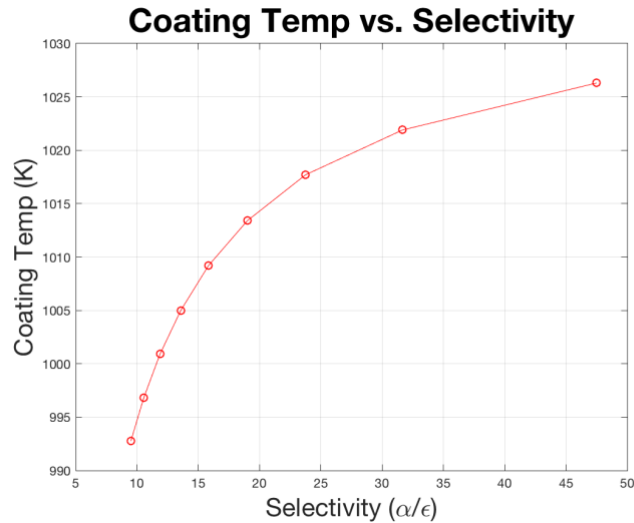


Figure 7: Coating temperature variation as a function of selectivity, showing increases in temperature as the quality of the coating increases.

Using the chosen selectivity of 19 results in a coating temperature of 1014 K. However, drastically increasing the selectivity to 47.5 only increases temperature to 1026 K. This ~1% improvement in coating temperature is not worth the immense effort required in increasing the selectivity to cutting-edge levels.

Clearly, absorption coating optimization can drastically improve collector performance and help achieve high temperatures even without high concentration. Optimizing cutoff frequency seems to provide greater benefits than improving selectivity.

Conclusions

A numerical model of high-temperature concentrated solar collector was created and optimized in this study. The collector consists of an absorber with a solar selective absorption coating deposited on a copper plate, tubes with fluid flow of CH_4 and CO_2 at the inlet, a packed catalyst bed to react the inlet gases to form H_2 and CO , a steel bulkhead to allow inlet and outlet tubes to pass through, and a glass cover to create a vacuum insulation.

Physics interfaces were used to model heat transfer, fluid flow, and chemical reaction, and multiphysics interfaces were used to properly couple terms between these interfaces. Surface-to-surface radiation with solar/ambient split spectrum was used to model radiative heat transfer, which was especially important for the selective coating. Weakly compressible flow was used to model laminar flow, due to the density differences caused by temperature difference and reaction. Transport of concentrated species and chemistry interfaces were both used to model chemical reaction using Arrhenius expressions for rate constants.

The model was optimized by considering various materials for the tubes connecting the absorber to the steel bulkhead, improving insulation while still retaining a proper seal. The packed catalyst bed was modeled as a control volume with homogeneous chemical reaction, and the values in the Arrhenius equation were tuned to match experimental data for dry methane reforming. Finally, the absorption coating optical

properties were optimized to increase coating temperature. Adjusting the cutoff wavelength between high solar absorption and low ambient emissivity drastically improved performance.

Future work includes conducting a steady state analysis for coating temperature and CH₄/CO₂ conversion as a function of flowrate and CR. Additionally, an incorporation of the microfluidics module would model vacuum influence on collector temperature. Our final goal is to fabricate of physical collector and compare experimental results from this collector to the simulated results.

References

- [1] L. L. Kazmerski, "Solar photovoltaics R&D at the tipping point: A 2005 technology overview," *Journal of Electron Spectroscopy and Related Phenomena*, vol. 150, no. 2-3, pp. 105-135, 2006.
- [2] M. A. Green, K. Emery, Y. Hishikawa and W. Warta, "Solar cell efficiency tables (version 37)," *Progress in Photovoltaics*, vol. 19, pp. 84-92, 2010.
- [3] M. M. Thackeray, C. Wolverton and a. E. D. Isaacs, "Electrical energy storage for transportation—approaching the limits of, and going beyond, lithium-ion batteries," *Energy and Environmental Science*, vol. 5, pp. 7854-7863, 2012.
- [4] V. Quaschnig, "Technical and economical system comparison of photovoltaic and concentrating solar thermal power systems depending on annual global irradiation," *Solar Energy*, vol. 77, no. 2, pp. 171-178 , 2004.
- [5] J. Moon, D. Lu, B. V. Saders, T. K. Kim, S. D. Kong, S. Jin, R. Chen and Z. Liu, "High performance multi-scaled nanostructured spectrally selective coating for concentrating solar power," *Nano Energy*, vol. 8, pp. 238-246 , 2014.
- [6] C. Kennedy, "Review of Mid- to High- Temperature Solar Selective Absorber Materials," National Renewable Energy Laboratory , Golden, 2002.
- [7] V. Garimella and Z. Y. Suresh, "Thermal analysis of solar thermal energy storage in a molten-salt thermocline," vol. 84, no. 6, pp. 974-985, 2010.
- [8] O. o. E. E. & R. ENERGY, "Hydrogen Production: Natural Gas Reforming," Department of Energy, 2010. [Online]. Available: <https://www.energy.gov/eere/fuelcells/hydrogen-production-natural-gas-reforming>.
- [9] S. Arora and R. Prasad, "An overview on dry reforming of methane: strategies to reduce carbonaceous deactivation of catalysts," *The Royal Society of Chemistry*, vol. 6, p. 108668–108688, 2016.
- [10] S. T. Oyama, PelinHacarlioglu, YunfengGu and D. Lee, "Dry reforming of methane has no future for hydrogen production: Comparison with steam reforming at high pressure in standard and membrane reactors," *International Journal of Hydrogen Energy*, vol. 37, no. 13, pp. 10444-10450 , 2012.
- [11] F. Bustamante, R. Enick, K. Rothenberger, B. Howard, A. Cugini, M. Ciocco and B. Morreale, "High-Temperature Kinetics of the Homogeneous Reverse Water–Gas Shift Reaction," *American Institute of Chemical Engineers*, vol. 50, no. 5, pp. 1028-1041, 2004.

- [12] Igor Luisetto, S. Tuti and E. D. Bartolomeo, "Co and Ni supported on CeO₂ as selective bimetallic catalyst for dry reforming of methane," *International Journal of Hydrogen Energy*, vol. 37, no. 21, pp. 15992-15999, 2012.
- [13] D. Real, R. Johnston, J. Lauer, A. Schicho and N. Hotz, "Novel non-concentrating solar collector for intermediate-temperature energy capture," *Solar Energy*, vol. 108, pp. 421-431, 2014.
- [14] U. Olsbye, T. Wurzel and a. L. Mleczko, "Kinetic and Reaction Engineering Studies of Dry Reforming of Methane over a Ni/La/Al₂O₃ Catalyst," *Industrial and Engineering Chemistry Research*, vol. 36, no. 12, p. 5180–5188, 1997.
- [15] M. Soria, C. Mateos-Pedrero, A. Guerrero-Ruiz and I. Rodríguez-Ramos, "Thermodynamic and experimental study of combined dry and steam reforming of methane on Ru/ ZrO₂-La₂O₃ catalyst at low temperature," *International Journal of Hydrogen Energy*, vol. 36, no. 23, pp. 15212-15220, 2011.